

Visual field defects and retinal nerve fiber layer damage in buried optic disc drusen: a new insight

Brenda Nana Wandji¹, Artémise Dugauquier², Adèle Ehongo²

¹Faculty of Medicine, Université Libre de Bruxelles, Brussels 1070, Belgium

²Department of Ophthalmology, Erasme Hospital, Brussels 1070, Belgium

Correspondence to: Brenda Nana Wandji. Faculty of Medicine, Université Libre de Bruxelles, Brussels 1070, Belgium. Brenda.Nana.Wandji@ulb.be

Received: 2022-04-11 Accepted: 2022-07-05

Abstract

• **AIM:** To assess the association between buried optic disc drusen (BODD) location using spectral-domain optical coherence tomography (SD-OCT) and the location of associated visual field defects (VFD) using the Garway-Heath mapping.

• **METHODS:** This monocentric retrospective cross-sectional study was led at the authors' institution. Adult patients diagnosed with BODD who had complete records with a reliable Humphrey® 24-2 visual field, macular, and papillary OCT were enrolled. Fisher's exact test was used to measure the association between BODD location and VFD distribution according to Garway-Heath's mapping.

• **RESULTS:** Totally 20 eyes of 15 patients were included (60% females). The median age (interquartile range) was 63 (43)y and the median best corrected visual acuity (BCVA) was -0.08 (0.08) log MAR. BODD were mostly located in zones A, E, and F. The minimal rim width (MRW) was globally preserved. The retinal nerve fiber layer (RNFL) was predominantly altered in zones D, E, and F. There was a significant correlation between BODD location and that of RNFL alterations in zones D ($P=0.03$) and E ($P=0.025$); Moreover, the presence of BODD in the E zone was significantly related to damaged RNFL in the neighbouring sectors D and F ($P=0.012$; $P=0.02$ respectively). Sixty-three percent (12/19) of visual fields were abnormal and there was a significant match ($\Phi=0.7$, $P=0.009$) between drusen location and VFD only in zone D.

• **CONCLUSION:** BODD do not only affect young patients and can be more harmful than usually expected, as we found VFD in 63% of cases. There is a correspondence between BODD location, RNFL damage, and VFD distributions. The presence of BODD induces the overestimation of MRW,

thereby disrupting its sensitivity as an early indicator of ganglion fibers damage.

• **KEYWORDS:** buried optic disc drusen; visual field; spectral-domain optical coherence tomography; Garway-Heath mapping; retinal nerve fiber layer

DOI:10.18240/ijo.2022.10.12

Citation: Nana Wandji B, Dugauquier A, Ehongo A. Visual field defects and retinal nerve fiber layer damage in buried optic disc drusen: a new insight. *Int J Ophthalmol* 2022;15(10):1641-1649

INTRODUCTION

Optic disc drusen (ODD) are acellular deposits made of mucopolysaccharides, calcium and nucleic acids located at the prelaminar zone of the optic nerve head (ONH)^[1]. Their pathophysiology is not well known but it is commonly admitted that an axonal calcium flow reduction leading to extracellular calcic collections could be the main mechanism^[2-3]. ODD have a global prevalence of 0.9%-2.4% and are more common in Caucasians and females^[4-5]. There may also be a genetic component, explaining increased intrafamilial occurrence^[6]. ODD is usually asymptomatic. However, up to 10% of patients may report transient visual obscuration^[7] and 88.3% of patients may develop associated visual field defects (VFD)^[8-10]. ODD are usually located in the nasal sectors of the papilla^[11-12]; they are classified either as visible or buried depending on the fact that they are clearly detected or not by ophthalmoscopy^[2]. Visible ODD have a typical nodular presentation or appear as polycyclic and blurred distortions of the optic disc margins^[10]. Buried optic disc drusen (BODD), do not have that typical aspect. They can induce a papillary bulge, often confused with papilledema but the ophthalmoscopic examination can also be strictly normal^[2,13]. BODD are therefore insidious because they can be underdiagnosed or confused with pathologies such as normal tension glaucoma (NTG) or papilledema, leading thus to unnecessary investigations^[13-14]. BODD are easily detected using the latest optical coherence tomography (OCT) technologies such as swept source-OCT (SS-OCT) and enhanced depth imaging-OCT (EDI-OCT)^[15-16]. BODD are more commonly found in children and a transition period is described in adolescence during which BODD exteriorize^[2,5].

The alterations caused by BODD on retinal nerve fiber layer (RNFL) and the impact on the visual field (VF) are controversial unlike visible ODD where the association is well known^[9,17]. The theory is that BODD are early-stage ODD that have not yet had time enough to exteriorize and cause damages^[9].

The relationship between VF patterns and their corresponding regions on the ONH is established^[18]. Using this correspondence, we assessed the correlation between the localization of BODD and their impact on the VF in adults. We suggest that drusen may trigger VFD by compressing RNFL and this damage would be more pronounced in adult patients.

SUBJECTS AND METHODS

Ethical Approval We obtained the approval of the Ethics Committee and that of the institutional board of Erasme Hospital. We have ensured that our study was conducted in accordance with the fundamental principles of medical research as set out in the Declaration of Helsinki. The hospital where our study was conducted is an academic institution that applies the opting-out policy; therefore, all patients admitted give their consent to the hospital for further use of their records for research purpose.

Study Design We carried out a retrospective hospital-based cross-sectional descriptive study in the Glaucoma Clinic of the Ophthalmology Department at Erasme Hospital in Brussels, Belgium. Patients aged at least 18 years old diagnosed with BODD, who had complete records and reliable VF were enrolled. We excluded patients with low vision, age-related macular degeneration, retinitis pigmentosa or any other lesion potentially responsible of VFD.

Sampling The sampling was done with consecutive subjects for whom BODD diagnosis was made over a 3-year period from November 2018 to December 2021.

Study Procedure Data were collected from the files of patients who benefitted from a comprehensive ophthalmic examination including medical history, measurement of their refractive error, best corrected visual acuity (BCVA), intra-ocular pressure (IOP) using Goldman applanation tonometer fundus examination and pictures with a non-mydratic retinal camera Visucam 224[®] (Carl Zeiss Meditec AG, Jena, Germany), automated 24-2 VF using the SITA standard mode of the Humphrey[®] Field Analyzer 3 (Carl Zeiss Meditec AG, Jena, Germany) and spectral domain OCT (SD-OCT) with Spectralis[®] OCT model S3300 (Heidelberg Engineering GmbH, Heidelberg, Germany).

OCT Data Collection ODD were considered visible if they had a typical nodular or polycyclic appearance on ophthalmoscopy^[10] (Figure 1A) and these eyes were thus non included. Otherwise, they were considered buried. The diagnosis of BODD was made using the glaucoma module of

Spectralis[®] which provides 48 radial sections centred on the papilla. BODD were identified as round hypo reflective lesions with hyper reflective and irregular margins^[2] (Figure 1B-1D). We were careful not to confuse them with vessels which usually have regular margins and only appear on a single section^[19-20].

OCT Analysis One radial section out of four was analysed starting from the 12 o'clock position and read clockwise. In case of doubt, the interpretation was refined by reading the neighbouring section on both sides. Then, we made a transition from the hourly to the Garway-Heath distribution^[18] (Figure 1E). For both the RNFL and the minimal rim width (MRW), we used this all-set distribution provided by the Spectralis[®] after revision of the Bruch's membrane position.

To assess the predominantly nasal location of BODD^[11-12], we also assessed on the hourly slices, the orientation of the border tissue of Elschnig which is a fibro-astrocytic tissue that separates neural tissue from choroid in the neural canal. It was classified into two categories according to whether it is externally oblique or not from its junction with the sclera to that with Bruch's membrane: external oblique if its anterior end goes outwards in relation to the center of the optic nerve and non-external oblique otherwise^[21] (Figure 2A). We then classified the sections at the right eye into two sectors: "nasal" from 12:00 to 6:00 clockwise including the limits (6 and 12) and "temporal" from 6:00 to 12:00 clockwise. To obtain the corresponding mirror sections for the left eye, we made a symmetrical projection around the nasal axis (Figure 2B). "Temporal" data of right and left eyes for the border tissue obliquity were pooled together for each hourly location and the same for the "nasal" part (For example we combined the data from 3:00 of the right eye and 9:00 of the left eye which corresponded to the "nasal 3" sector while the data from 9:00 of the right eye and 3:00 of the left eye corresponding to the "temporal 3" sector).

The topography of BODD using SD-OCT was correlated to that of abnormal sectors for both the MRW and the RNFL. Likewise, the topography of abnormal sectors for MRW was correlated to that of abnormal sectors for the RNFL. A dissociation between the MRW and the RNFL in a sector was defined as normal MRW with damaged RNFL in that same sector or vice-versa.

Visual Field Assessment VF were considered reliable if they had a rate of false positives, false negatives, and fixation losses <20%. Unreliable VFs were excluded. Reliable VFs were then analyzed according to Anderson's criteria which can be summarized as follows: glaucoma hemifield test (GHT) outside normal limits; or pattern standard deviation (PSD) at a $P < 5\%$; or abnormal cluster. Abnormal cluster is a group of three or more non-edge points along the course of the nerve fiber within the same sector on the pattern deviation plot, all

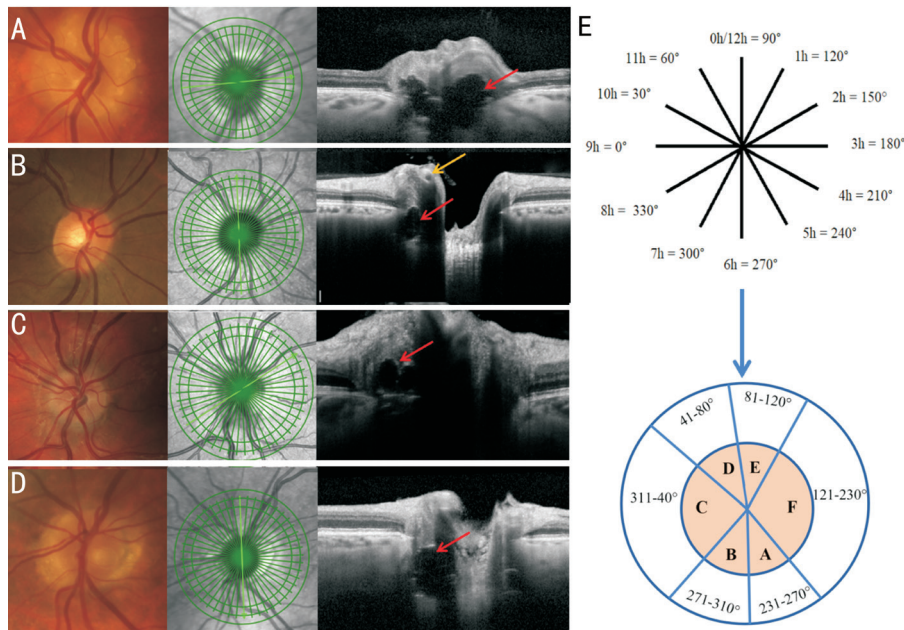


Figure 1 Fundus and OCT aspects of optic disc drusen (A-D) and translocation from hourly sectors to Garway-Heath zones (E) A: Visible optic disc drusen: multinodular aspect on funduscopy; B: Normal funduscopy hiding a buried optic disc drusen disclosed by SD-OCT as a round hypo reflective lesion with hyper reflective and irregular margins: the yellow arrow shows a vessel which is round, hypo reflective with hyper reflective regular margins; C: Buried optic disc drusen presenting with a pseudo papilledema aspect on funduscopy; D: Buried optic disc drusen presenting with peripapillary atrophy on funduscopy: based on exclusion criteria stated above, this eye was excluded as peripapillary atrophy is a confounding factor for visual field defects^[20]; E: Summary of our approach of transposition from hourly sectors on SD-OCT to Garway-Heath areas on a right eye; to obtain a mapping for a left eye, this figure is mirrored by the vertical line crossing the nose. SD-OCT: Spectral-domain optical coherence tomography.

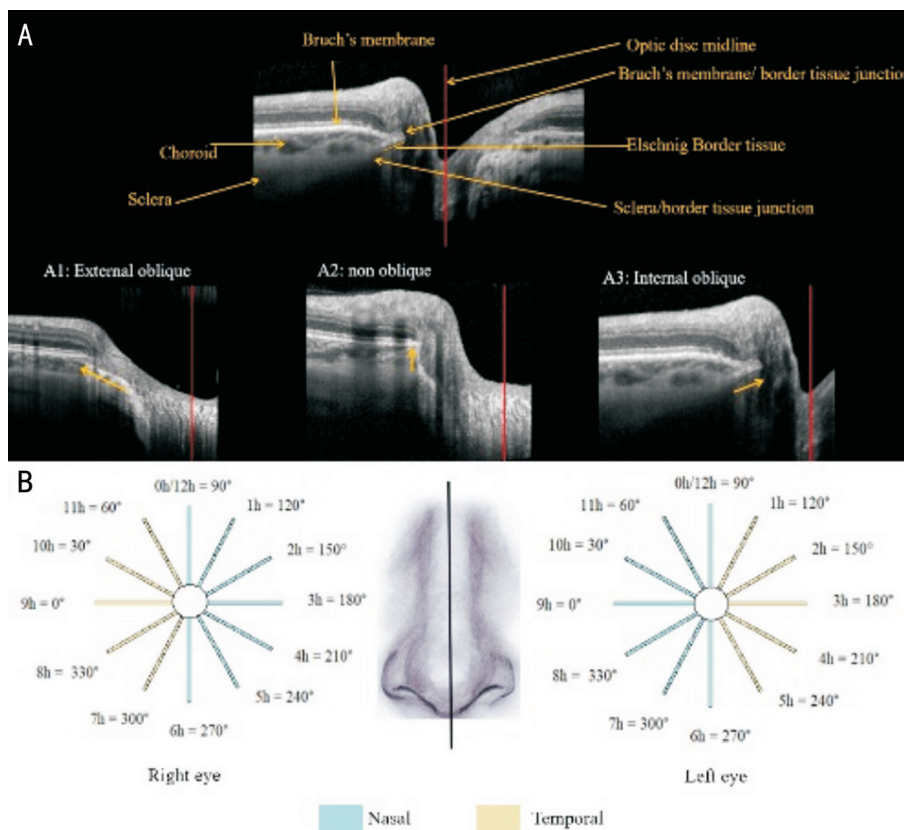


Figure 2 Representation of border tissue and right-left equivalent hourly sectors A: Border tissue orientation; A1: external oblique: anterior end goes outwards in relation to the center of the optic nerve and non-external oblique otherwise; A2 and A3: non external oblique (respectively non-oblique and internal oblique); B: Hourly sectors on right and left eyes.

of which are depressed at a $P < 5\%$ level with at least one of them depressed at a $P < 1\%$ level^[22]. Then clusters were listed in Garway-Heath's zones (Figure 3).

The topography of BODD using SD-OCT was correlated to VFD distribution according to Garway-Heath correspondence.

All data including VF were analyzed by two independent researchers (Dugauquier A and Ehongo A) and a third one (Nana Wandji B) independently validated their findings. In case of agreement, data were saved in an Excel sheet and in case of disagreement, they were reviewed collegially. If a doubt persisted, the data were excluded.

Statistical Analysis Statistical analysis was performed using Microsoft Office Excel and STATA SE 17 (64 bit) software. The qualitative variables were expressed in terms of frequencies, while the quantitative variables were expressed as median, interquartile range (IQR) and range. The Fisher's exact test was used to verify the associations between the different variables of interest because most expected counts were < 5 . We also used the Phi correlation coefficient for categorical variables to rate the strength of our correlation. We performed an exact logistic regression adjusting for elevated IOP (> 21 mm Hg) which influences VFD^[23-24]. The tests were considered significant for a P -value < 0.05 .

RESULTS

General Characteristics Twenty eyes of 15 patients, aged 19 to 76y (median \pm IQR: 63 \pm 43y), of which 9/15 (60%) females, were included. Patients' distribution according to the age is shown in Figure 4A. The optic disc aspect was strictly normal in 19 out of 20 eyes (95%); We had one case of pseudo papilledema. One eye with peripapillary atrophy and BODD was excluded as the former may be related to VFD^[20]. BODD were found in 12 left eyes (60%) and in 8 right eyes (40%); They were bilateral in 6 (40%) patients. Circumstances of diagnosis were usually related to glaucoma (Figure 4B). The other general characteristics are summarized in Table 1.

SD-OCT Analysis BODD were mostly found in areas A, E and F, corresponding to the nasal region (Figure 5A). RNFL was predominantly damaged in the D, E, and F zones (Figure 5B). MRW was slightly impaired (Figure 5C).

The border tissue obliquity was predominantly external in the temporal sectors while it was non external in the nasal sectors (Figure 6A). Figure 6B shows the association between BODD location and the orientation of the border tissue. There is less BODD in the temporal areas, where the border tissue is predominantly external oblique. This association was not statistically significant.

RNFL damage was significantly associated with BODD location in C, D and E areas; There was no statistically significant association between BODD location and MRW impairment (Table 2).

Table 1 General characteristics of the sample

General characteristics	Median (IQR)	Range
Age (y)	63 (43)	19 to 76
Refractive error in SE (D)	0 (2.37)	-6.25 to +3.00
BCVA (log MAR)	-0.08 (0.08)	-0.18 to 0.15
Intraocular pressure (mm Hg)	17.5 (5)	12 to 38
Central cornea thickness (μ m)	558 (34.5)	496 to 623
Mean deviation (dB)	-1.65 (3.56)	-14.20 to 1.07
PSD (dB)	2.26 (2.96)	1.27 to 14.30
VFI	0.98 (0.06)	0.54 to 1

SE: Spherical equivalent; BCVA: Best corrected visual acuity; PSD: Pattern standard deviation; VFI: Visual field index; IQR: Interquartile range; logMAR: Logarithm of the minimum angle of resolution; dB: Decibel.

After adjusting for high IOP, the association between the presence of BODD and RNFL damage was still significant in D ($P=0.03$) and E ($P=0.025$; Table 3). Moreover, BODD located in E were significantly associated with damaged RNFL in neighboring sectors D ($P=0.012$) and F ($P=0.02$; Table 3).

A statistically significant MRW/RNFL dissociation was noticed on the A, E and F Garway-Heath areas with a damaged RNFL meanwhile MRW was still normal (Table 4). Figure 7 shows the distribution of MRW-RNFL dissociation by Garway-Heath areas (Figure 7A-7B). A case of dissociation is also illustrated (Figure 7C1-7C4).

Visual Field Analysis We excluded one VF because it did not meet the reliability criteria. The overall positive rate for Anderson criteria was 63% (12/19; Figure 8A). Clusters were mostly located in the B (31.6%), D (21%), and E (26.3%) Garway-Heath's areas (Figure 8B).

There was a statistically significant association between the location of BODD and the location of clusters only in zone D. This association remained significant after adjustment for high IOP ($P=0.009$; Table 5). Figure 9 illustrates one case of structure-function correspondence.

The further away from the F-zone, the less BODD are present. The RNFL damage also follows this pattern but with a more spread-out distribution. When it comes to VFD, the areas with the most defects are those adjacent to the areas with the most BODD: areas B and E with the most VFDs are adjacent to areas A and F with the most BODD (Figure 10).

DISCUSSION

The median age at diagnosis in our study sample was 63y, which indicates a delay in diagnosis since BODD are asymptomatic. BODD are usually found in a younger population^[5,25], but our study did not include any patients under 18 years old. There was a slight female predominance, which is consistent with the literature^[9]. The mean visual acuity of our patients was nearly normal like the one in the study of Malmqvist *et al*^[9]. This could also play a role in the delayed diagnosis.

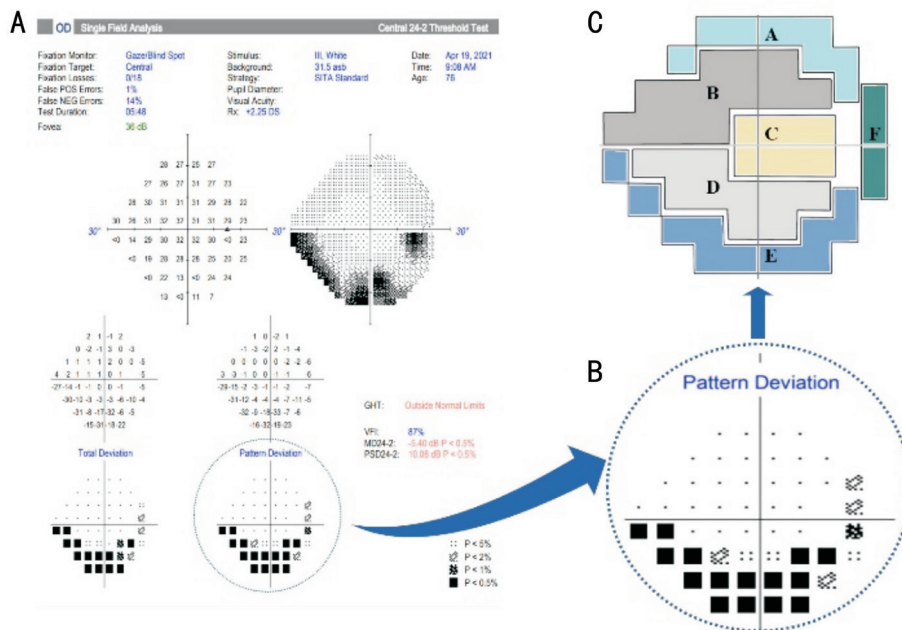


Figure 3 Transition of visual field data from the results sheet to the Garway-Heath mapping A: VF results sheet; B: Pattern deviation; C: Garway-Heath areas; the defects correspond to D, E, and F areas.

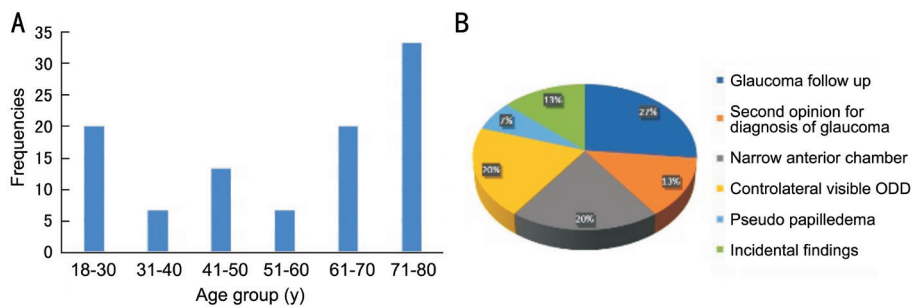


Figure 4 General characteristics A: Age distribution ($n=15$); B: Circumstances of diagnosis ($n=21$).

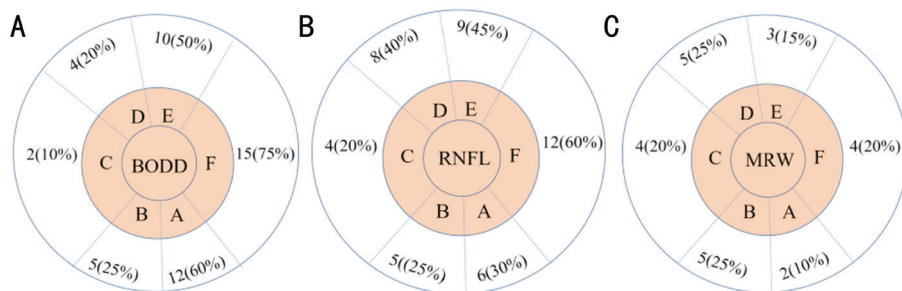


Figure 5 Distribution by Garway-Heath area A: BODD location; B: RNFL damage; C: MRW damage. The results presented here are those for right and left eyes combined by Garway-Heath sector. The mapping for a right eye is just used for simplification. BODD: Buried optic disc drusen location; RNFL: Retinal nerve fiber layer; MRW: Minimal rim width.

Table 2 Correspondence between BODD location, RNFL, and MRW damage

BODD location	RNFL and MRW damage location	RNFL damage			MRW damage		
		Phi	P	Fisher	Phi	P	Fisher
BODD A	Zone A	0.13	0.55	0.45	0.41	0.07	0.15
BODD B	Zone B	0.20	0.37	0.36	0.07	0.76	0.63
BODD C	Zone C	0.67	0.003 ^a	0.03 ^b	0.17	0.46	0.63
BODD D	Zone D	0.61	0.006 ^a	0.014 ^b	0.29	0.19	0.28
BODD E	Zone E	0.50	0.025 ^a	0.035 ^b	0.14	0.53	0.50
BODD F	Zone F	<0.001	0.999	0.69	<0.001	0.999	0.72

^aSignificant P-value; ^bSignificant Fisher exact test. BODD: Buried optic disc drusen location; RNFL: Retinal nerve fiber layer; MRW: Minimal rim width.

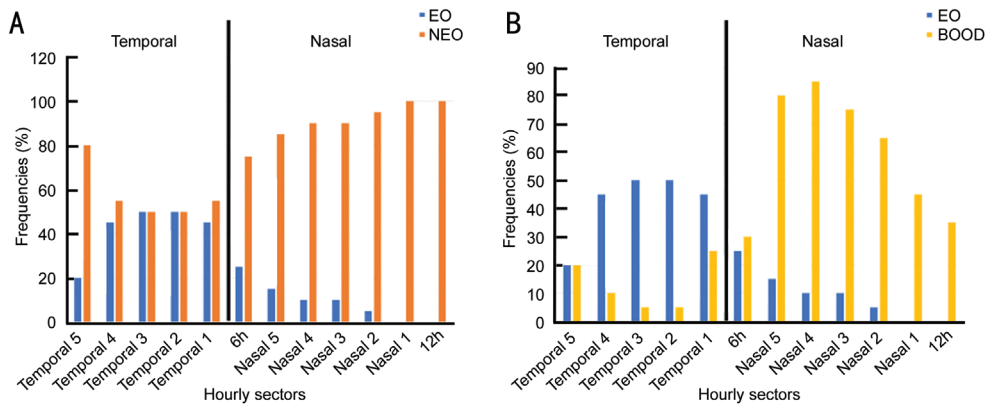


Figure 6 Border tissue orientation analysis A: Distribution of border tissue orientation; B: Association between external obliquity of border tissue and BOOD location. EO: External oblique; NEO: Non external oblique; BOOD: Buried optic disc drusen location.

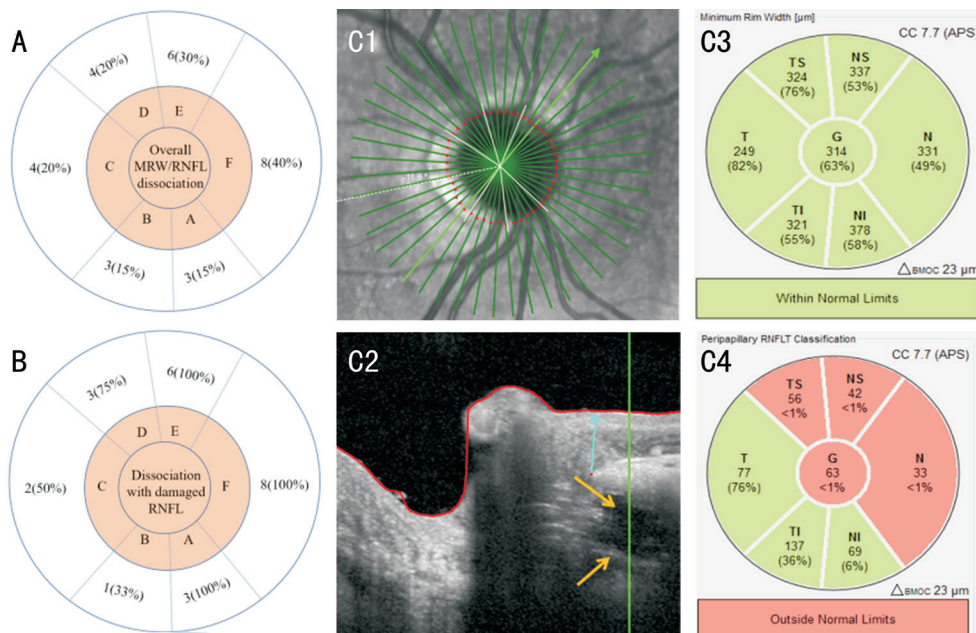


Figure 7 MRW/RNFL dissociation A: Summary of overall MRW/RNFL dissociation according to Garway-Heath areas. The dissociation is more prevalent in sectors D, E, and F. B: Distribution of the part of MRW/RNFL dissociation related to damaged RNFL. The cases of nasal dissociation are mainly due to damage of RNFL. C: Illustration of a case of dissociation in a right eye. This 76-year-old patient has bilateral BOOD discovered in the context of shallow anterior chamber work up, maximum IOP 10 mm Hg. C1: Hourly sectors with the cursor at 2 o'clock; C2: BOOD seen on SD-OCT; C3: Normal MRW; C4: Damaged RNFL in D, E and F Garway-Heath areas. BOOD: Buried optic disc drusen location; RNFL: Retinal nerve fiber layer; MRW: Minimal rim width; IOP: Intraocular pressure.

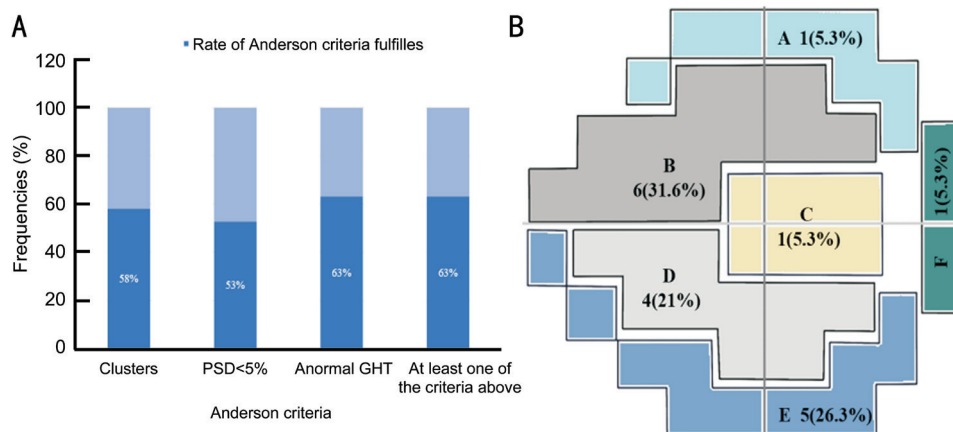


Figure 8 Visual field deficits A: Rate of Anderson criteria fulfilled ($n=19$). Clusters were found in 58% (11/19) of eyes, the PSD was <5% in 53% (10/19) of eyes and 63% of the eyes (12/19) had an abnormal GHT. B: Clusters proportion by Garway-Heath zone. PSD: Pattern standard deviation; GHT: Glaucoma hemifield test.

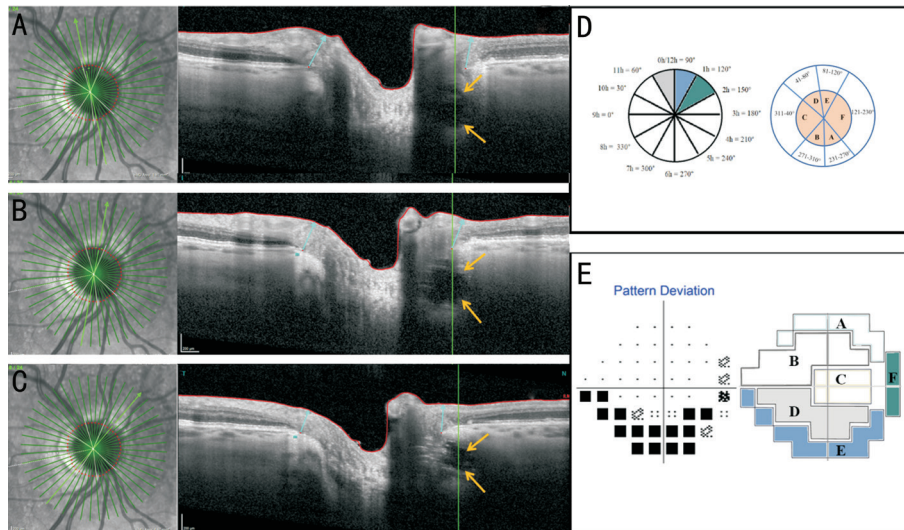


Figure 9 Right eye correspondence between BODD located in the D, E, and F Garway-Heath areas with clusters in D, E, and F on visual field In each line, the infrared image with OCT radial sections in the left shows the location and orientation of the slice disclosing the drusen. A-C: SD-OCT with BODD respectively at 11, 1, and 2 o'clock; D: Transposition from corresponding hourly sections to D, E, F Garway-Heath areas; E: Visual field of the same patient with defects on the D, E and F areas. The same patient illustrated in Figure 7. BODD: Buried optic disc drusen location.

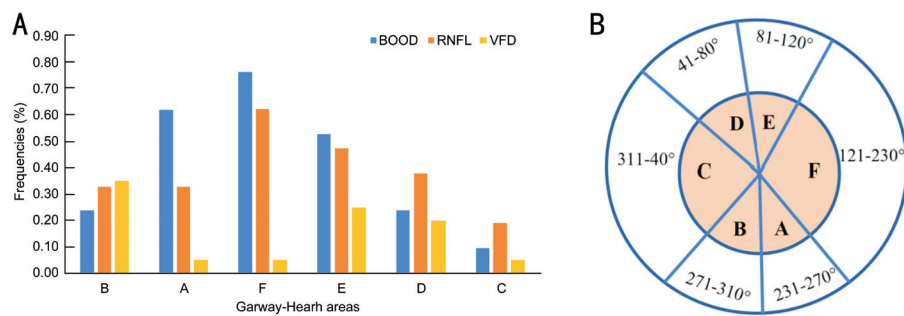


Figure 10 Overview of BODD, RNFL damage, and clusters distribution A: BODD, RNFL damage, and VFD distribution; B: Garway-Heath mapping. BODD: Buried optic disc drusen location; RNFL: Retinal nerve fiber layer; VFD: Visual field defects.

We found a bilateral BODD rate of 40%. We found no studies describing only the rate of bilaterality of BODD only. The papilla appeared normal in 95% of our sample, with the typical presentation of pseudo papilledema^[19] being found only in one case. This suggests that BODD are underdiagnosed, thus their true prevalence is underestimated. Nearly 60% of BODD included in our study were discovered during investigative assessment for pathologies related to glaucoma (narrow angle glaucoma work-up, 2nd opinion for glaucoma)^[26]. Therefore, BODD are a diagnosis to keep in mind when dealing with glaucoma^[14,27].

BODD were predominantly located in Garway-Heath sectors A, E and F, corresponding to the lower, upper, and middle nasal regions which is in accordance with those found by Sato *et al*^[11] and Teixeira *et al*^[12]. The orientation of the border tissue was mostly external oblique in the temporal region, where very few BODD were found. Although this association was not statistically significant, we suggest that this may explain

why BODD are more often found in the nasal area. This phenomenon has already been described in myopic eyes with external obliquity of the border tissue on the temporal side; The prelaminar optic nerve then tends to slide nasally, freeing the temporal part^[21]. Since the pathogenesis of BODD results from an alteration of axonal metabolism^[2], a more frequent number of BODD in the nasal area would then be related to the greater number of nerve fibers in this area due to the orientation of the border tissue. So far, no study has provided a hypothesis on the predominantly nasal localization of BODD.

We found an association in the location of BODD and RNFL damage (upper nasal and upper temporal) in Garway-Heath zones D and E, suggesting that BODD are not that harmless. This finding is quite innovative since in the literature, BODD seem not to cause RNFL alterations compared to ODD^[9,17]. It has been hypothesized that BODD are early-staged drusen, not present long enough to damage nerve fibers^[9] and also, that the outer walls of BODD are less calcified than those of ODD, making the former less harmful^[28].

Table 3 Correspondence between BODD location and RNFL damage adjusted for high IOP (exact logistic regression)

Independent variables	RNFL damage location		P
	OR	CI	
	RNFL C (n=20, n _{RNFLC} =4, n _{HIOP} =7)		
BODD C	14.44	0.83, +∞	0.07
High IOP	5.59	0.40, +∞	0.19
	RNFL D (n=20, n _{RNFLD} =8, n _{HIOP} =7)		
BODD D	11.63	1.24, +∞	0.03 ^a
High IOP	1.91	0.10, 36	0.97
	RNFL E (n=20, n _{RNFLE} =9, n _{HIOP} =7)		
BODD E	10.67	1.3, +∞	0.025 ^a
High IOP	4.39	0.47, +∞	0.21
	RNFL D (n=20, n _{RNFLD} =8, n _{HIOP} =7)		
BODD E	13.35	1.65, +∞	0.012 ^a
High IOP	2.48	0.24, +∞	0.38
	RNFL F (n=21, n _{RNFLF} =12, n _{HIOP} =7)		
BODD E	21.8	1.41, 1646.5	0.02 ^a
High IOP	2.8	0.15, 205.93	0.84

^aSignificant P-value. BODD: Buried optic disc drusen location; RNFL: Retinal nerve fiber layer; OR: Odds ratio; CI: Confidence interval; HIOP: High intraocular pressure.

Table 4 RNFL damage in MRW/RNFL dissociation

MRW/RNFL dissociation	RNFL damage location	Phi correlation	P	Fisher
Zone A	RNFL A	0.64	0.004 ^a	0.018 ^b
Zone B	RNFL B	0.08	0.72	0.6
Zone C	RNFL C	0.38	0.09	0.16
Zone D	RNFL D	0.35	0.11	0.255
Zone E	RNFL E	0.72	0.001 ^a	0.002 ^b
Zone F	RNFL F	0.67	0.003 ^a	0.004 ^b

^aSignificant P-value; ^bSignificant Fisher exact test. BODD: Buried optic disc drusen location; RNFL: Retinal nerve fiber layer; MRW: Minimal rim width.

Table 5 Correspondence between clusters' location and drusen's location

BODD location	Cluster's location	Phi correlation	P	Fisher
Zone A	Clusters A	0.31	0.18	0.37
Zone B	Clusters B	0.11	0.64	0.52
Zone C	Clusters C	0.08	0.72	0.89
Zone D	Clusters D	0.70	<0.001 ^a	0.004 ^b
Zone E	Clusters E	0.15	0.51	0.44
Zone F	Clusters F	0.14	0.54	0.73
		OR	CI	P
	Clusters D (n=19, n _{clusters D} =4, n _{HIOP} =7)			
Zone D		26.3	2.24, +∞	0.009 ^a
High IOP		1.67	0.04, +∞	0.75

^aSignificant P-value; ^bSignificant Fisher exact test. BODD: Buried optic disc drusen location; OR: Odds ratio; CI: Confidence interval; IOP: Intraocular pressure.

Interesting, we found that the lesions caused by BODD on the RNFL are not only restricted in the area where the drusen is located but also afar. This could be explained by a possible

mass effect away on the nerve fibers rather than at the epicenter of the drusen. A similar process occurs in case of intracranial expansive pathology that causes deficits in the ipsilateral and contralateral cerebral hemisphere also^[29].

The MRW was hardly damaged in most of our patients. This was also highlighted by Poli *et al*^[30]. Moreover, we had a significant RNFL/MRW dissociation with damaged RNFL. As suggested by Poli *et al*^[30], we suggest that the contribution of the MRW as indicator of fiber nerve damage is quite limited in case of morphological papillary abnormality such as BODD. The measurement between the internal limiting membrane and Bruch's membrane is overestimated by the space taken by BODD^[27,30].

This is a major difference with early glaucomatous lesions where alterations are first flagged by MRW^[31]. The 63% of our patients had an abnormal VF. This is slightly higher than the rate found by Malmqvist *et al*^[9] in patients with BODD which was 54.6% but this was remarkably high compared to the result found by Katz *et al*^[17], who had a rate of 5% of VFD in patients with BODD. This can be explained by the higher average age of our population which was 63y. Katz *et al*^[17] and Malmqvist *et al*^[9] in their studies had a mean age of patients with BODD of 35 and 35.4y respectively. In our subjects, this would have given BODD more time to damage nerve fibers.

The defects were predominantly found in areas B, D and E; contrary to what was found by Malmqvist *et al*^[9] and Noval *et al*^[25] which had a predominance of nasal defects. However, Katz *et al*^[17] found that BODD caused inferior arciform scotomas. This corresponds to Garway-Heath areas D and E which was also predominant in our study. The presence of defects in B could be explained by the possibility of a mass effect as for RNFL damages. BODD being less calcified^[9] would be more damaging by mass effect and therefore remotely whereas visible ODD would alter the fibres locally because of their calcifications.

Moreover, we observed a correspondence between the location of BODD and the presence of clusters in sector D (superior temporal). This correspondence was known in visible ODD but not in BODD^[5,9].

The sample size was small. Our study was monocentric, and retrospective and we did not have a control group. Since our participants were recruited at the Glaucoma Clinic, this is a potential selection bias. However, we focused on BODD, which are neglected in most studies and considered benign. We showed that VFD are also present in BODD. We did the study with a more specific distribution according to the Garway-Heath areas.

We can conclude that BODD do not affect only young patients and can be more harmful than usually expected, as VFD are present in 63% of cases. There is a correspondence between BODD location, RNFL damage, and VFD. When dealing with

BODD, RNFL status is a better indicator of ganglion fiber damage compared to MRW unlike glaucoma. We suggest there is a possible remote nerve fiber damage, and the border tissue orientation would be a hypothesis explaining the preferential nasal location of the BODDs. Those assumptions could be the subject of further studies.

ACKNOWLEDGEMENTS

The authors would like to thank Mr. Bouziotis Jason, Biomedical Research Department, Erasme Hospital, for his advice in biostatistics.

Conflicts of Interest: Nana Wandji B, None; Dugauquier A, None; Ehongo A, None.

REFERENCES

- 1 Friedman AH, Beckerman B, Gold DH, Walsh JB, Gartner S. Drusen of the optic disc. *Surv Ophthalmol* 1977;21(5):373-390.
- 2 Allegrini D, Pagano L, Ferrara M, Borgia A, Sorrentino T, Montesano G, Angi M, Romano MR. Optic disc drusen: a systematic review: up-to-date and future perspective. *Int Ophthalmol* 2020;40(8):2119-2127.
- 3 Palmer E, Gale J, Crowston JG, Wells AP. Optic nerve head drusen: an update. *Neuroophthalmology* 2018;42(6):367-384.
- 4 Serpen JY, Prasov L, Zein WM, Cukras CA, Cunningham D, Murphy EC, Turriff A, Brooks BP, Huryn LA. Clinical features of optic disc drusen in an ophthalmic genetics cohort. *J Ophthalmol* 2020;2020:5082706.
- 5 Hamann S, Malmqvist L, Costello F. Optic disc drusen: understanding an old problem from a new perspective. *Acta Ophthalmol* 2018;96(7):673-684.
- 6 Antcliff RJ, Spalton DJ. Are optic disc drusen inherited? *Ophthalmology* 1999;106(7):1278-1281.
- 7 Ahmed H, Khazaeni L. Optic Disc Drusen. In: StatPearls. Treasure Island (Florida): StatPearls Publishing; 2022.
- 8 Sustronck P, Nguyen DT, Jean-Charles A, David T, Merle H. Visual field defects due to optic nerve drusen in Afro-Caribbean patients: a case series of 16 eyes. *J Fr Ophthalmol* 2021;44(7):989-994.
- 9 Malmqvist L, Wegener M, Sander BA, Hamann S. Peripapillary retinal nerve fiber layer thickness corresponds to drusen location and extent of visual field defects in superficial and buried optic disc drusen. *J Neuroophthalmol* 2016;36(1):41-45.
- 10 Wilkins JM, Pomeranz HD. Visual manifestations of visible and buried optic disc drusen. *J Neuroophthalmol* 2004;24(2):125-129.
- 11 Sato T, Mrejen S, Spaide RF. Multimodal imaging of optic disc drusen. *Am J Ophthalmol* 2013;156(2):275-282.e1.
- 12 Teixeira FJ, Marques RE, Mano SS, Couceiro R, Pinto F. Optic disc drusen in children: morphologic features using EDI-OCT. *Eye (Lond)* 2020;34(9):1577-1584.
- 13 Razek AAKA, Batouty N, Fathy W, Bassiouny R. Diffusion tensor imaging of the optic disc in idiopathic intracranial hypertension. *Neuroradiology* 2018;60(11):1159-1166.
- 14 Rosdahl JA, Asrani S. Glaucoma masqueraders: diagnosis by spectral domain optical coherence tomography. *Saudi J Ophthalmol* 2012;26(4):433-440.
- 15 Gise R, Gaier ED, Heidary G. Diagnosis and imaging of optic nerve head drusen. *Semin Ophthalmol* 2019;34(4):256-263.
- 16 Guo XH, Wu YJ, Wu YH, Liu H, Ming S, Cui HP, Fan K, Li SY, Lei B. Detection of superficial and buried optic disc drusen with swept-source optical coherence tomography. *BMC Ophthalmol* 2022;22(1):219.
- 17 Katz BJ, Pomeranz HD. Visual field defects and retinal nerve fiber layer defects in eyes with buried optic nerve drusen. *Am J Ophthalmol* 2006;141(2):248-253.e1.
- 18 Garway-Heath DF, Poinoosawmy D, Fitzke FW, Hitchings RA. Mapping the visual field to the optic disc in normal tension glaucoma eyes. *Ophthalmology* 2000;107(10):1809-1815.
- 19 Khonsari RH, Wegener M, Leruez S, Cochereau I, Milea D. Optic disc drusen or true papilledema? *Rev Neurol (Paris)* 2010;166(1):32-38.
- 20 Lee JY, Lee JE, Kwon J, Shin JW, Kook MS. Topographic relationship between optic disc torsion and β -zone peripapillary atrophy in the myopic eyes of young patients with glaucomatous-appearing visual field defects. *J Glaucoma* 2018;27(1):41-49.
- 21 Sawada Y, Araie M, Shibata H, Ishikawa M, Iwata T, Yoshitomi T. Optic disc margin anatomic features in myopic eyes with glaucoma with spectral-domain OCT. *Ophthalmology* 2018;125(12):1886-1897.
- 22 Anderson DR, Patella VM. *Automated Static Perimetry*. 2nd edition. USA: Mosby; 1999.
- 23 Oliveira-Ferreira C, Leuzinger-Dias M, Tavares-Ferreira J, Faria O, Falcão-Reis F. The relationship between intraocular pressure and optic nerve structural and functional damage in patients with optic nerve head drusen. *Neuroophthalmology* 2019;44(5):290-293.
- 24 Nolan KW, Lee MS, Jalalizadeh RA, Firl KC, Van Stavern GP, McClelland CM. Optic nerve head drusen: the relationship between intraocular pressure and optic nerve structure and function. *J Neuroophthalmol* 2018;38(2):147-150.
- 25 Noval S, Visa J, Contreras I. Visual field defects due to optic disk drusen in children. *Graefes Arch Clin Exp Ophthalmol* 2013;251(10):2445-2450.
- 26 Razeghinejad MR, Myers JS. Contemporary approach to the diagnosis and management of primary angle-closure disease. *Surv Ophthalmol* 2018;63(6):754-768.
- 27 Mardin C. Optical coherence tomography in glaucomas: tips and tricks. *Klin Monbl Augenheilkd* 2020;237(4):539-551.
- 28 Sahin A, Cingü AK, Ari S, Cinar Y, Çaça I. Bilateral optic disc drusen mimicking papilledema. *J Clin Neurol* 2012;8(2):151-154.
- 29 Shi E, Shi KB, Qiu SF, Sheth KN, Lawton MT, Ducruet AF. Chronic inflammation, cognitive impairment, and distal brain region alteration following intracerebral hemorrhage. *FASEB J* 2019;33(8):9616-9626.
- 30 Poli M, Colange J, Goutagny B, Sellem E. Glaucoma and optic nerve drusen: limitations of optic nerve head OCT. *J Fr Ophthalmol* 2017;40(7):542-546.
- 31 Taniguchi EV, Paschalis EI, Li DJ, Nouri-Mahdavi K, Brauner SC, Greenstein SH, Turalba AV, Wiggs JL, Pasquale LR, Shen LQ. Thin minimal rim width at Bruch's membrane opening is associated with glaucomatous paracentral visual field loss. *Clin Ophthalmol* 2017;11:2157-2167.